

A peer-reviewed version of this preprint was published in PeerJ on 26 March 2015.

[View the peer-reviewed version](#) (peerj.com/articles/858), which is the preferred citable publication unless you specifically need to cite this preprint.

Leinweber K, Kroth PG. 2015. Capsules of the diatom *Achnanthidium minutissimum* arise from fibrillar precursors and foster attachment of bacteria. PeerJ 3:e858 <https://doi.org/10.7717/peerj.858>

Capsules of the diatom *Achnanthidium minutissimum* arise from fibrillar precursors and foster attachment of bacteria

Katrin Leinweber, Peter Kroth

Achnanthidium minutissimum is a benthic diatom that may form biofilms on submerged, aquatic surfaces. Within these biofilms, *A. minutissimum* cells produce extracellular structures which facilitate substrate adhesion, such as stalks and capsules. Both consist of extracellular polymeric substance (EPS), but the microstructure and development stages of the capsules are so far unknown, despite a number of hypotheses about their function, including attachment and protection. We coupled scanning electron microscopy (SEM) to bright-field microscopy (BFM) and found that *A. minutissimum* capsules mostly possess an unstructured surface. However, capsule material that was mechanically stressed by being stretched between or around cells displayed fibrillar substructures. Fibrils were also found on the frustules of non-encapsulated cells, implicating that *A. minutissimum* capsules may develop from fibrillar precursors. Energy-dispersive X-ray (EDX) spectroscopy revealed that the capsule material contains little to no silicon, suggesting that the capsule does not arise from the cell wall. We furthermore show that bacteria attach preferentially to capsules, instead of non-encapsulated *A. minutissimum* cells, which supports the idea that capsules mediate diatom-bacteria interactions.

1 Authors

2 **Katrin Leinweber* and Peter G. Kroth***

3 * Biology Department, University of Konstanz, Germany

4 corresponding author:

5 Katrin Leinweber

6 Universität Konstanz

7 Postbox/Fach 611

8 78457 Konstanz

9 Germany

10 0049 7531 88 2782

11 katrin.leinweber@uni-konstanz.de

12 Introduction

13 Diatoms (Bacillariophyceae) are among the most productive photoautotrophic, aquatic micro-
14 organisms. They contribute an estimated 40-45% to the net primary production (NPP) of the
15 oceans (Mann, 1999), which themselves contribute approx. 45-50% to the global NPP (Field et
16 al., 1998). Additionally, diatoms are important for the biogeochemical cycling of silicon, due to
17 their ornate cell walls (called “frustules”) composed of biomineralised silica (Bradbury, 2004).
18 Cell division includes the separation of the two frustule parts (“thecae”) along a “girdle” region.
19 Each daughter cell then complements its inherited epitheca with a newly synthesised, smaller
20 hypotheca. Within these thecae, slits (called “raphes”) and pores may be present, facilitating the
21 secretion of extracellular polymeric substances (EPS) (Wetherbee et al., 1998; Wang et al., 2000).
22 This in turn conveys substrate attachment and motility to benthic diatoms, which often form
23 biofilms with other photoautotrophic algae, as well as heterotrophic bacteria (Buhmann, Kroth &
24 Schleheck, 2012).

25 The diatom *Achnanthidium minutissimum* (renamed from *Achnanthes minutissima* by
26 (Czarnecki & Edlund, 1995)) colonises the littoral zone of Lake Constance. It represents a
27 dominant species complex of early colonisers (Johnson, Tuchman & Peterson, 1997), forming
28 epilithic biofilms in association with a variety of satellite bacteria (Bahulikar, 2006). These
29 bacteria may influence the production of extracellular polymeric substances (EPS) by the diatom
30 (Bruckner et al., 2008, 2011). Similarly to the rhizosphere of terrestrial environments (composed
31 largely of fungi and bacteria associated with plant roots), a “phycosphere” has been defined as the
32 space surrounding algal cells including the multitude of inter-kingdom interactions between
33 bacteria and algae (Bell, Lang & Mitchell, 1974). EPS secretion is of ecological and
34 biogeographical relevance contributing for instance to the stabilisation of sediments (Cyr &
35 Morton, 2006; Lubarsky et al., 2010). Studying biofilm formation can therefore assist in the
36 understanding of shore- and coast-line erosion as a result of climate-related changes (see section
37 3.2.1 of (Widdows & Brinsley, 2002) plus references therein). At the same time diatom settlement
38 is one of the major causes of biofouling of man-made machinery in aquatic applications (Molino
39 & Wetherbee, 2008).

40 *A. minutissimum* is an excellent model for studying diatom biofilms, because this alga is
41 abundant *in natura* (Patrick & Reimer, 1966; Krammer K & Lange-Bertalot H, 1991) and can be
42 cultivated in the laboratory both as “xenic” biofilms (Myklestad et al., 1989) and “axenic”

43 suspension cultures (Windler et al., 2014b). Xenic cultures contain bacteria from the diatom's
44 natural habitat. Removal of these bacteria is possible (for example by antibiotic treatment) and
45 yields viable axenic cultures (Bruckner & Kroth, 2009; Windler, Gruber & Kroth, 2012).
46 Bacteria-free cultures allow the establishment of bioassays in order to study the interactions
47 between diatoms and bacteria, although potentially unwelcome long-term effects have to be taken
48 into account. For example, axenic growth can lead to a reduction of average cell size and to
49 frustule deformations (MacDonald, 1869; Pfitzer, 1871; Geitler, 1932; Windler et al., 2014a)

50 Our model species *A. minutissimum* forms biofilms and extracellular structures like and
51 capsules. Stalks have been investigated previously by transmission electron microscopy and
52 biochemical techniques to elucidate structural morphology and chemical composition (Daniel,
53 Chamberlain & Jones, 1987). Additionally, a phase model of diatom adhesion involving stalks
54 has been developed (Wang et al., 1997). Stalks may protrude from so called "basal pads" of
55 aggregated EPS at the apical valve faces within hours to a few days, thus elevating the cells
56 above the substrate. Capsule formation in *A. minutissimum* biofilms occurs later in the stationary
57 phase, is possibly triggered by bacterial influences, and may cement diatom attachment (Windler
58 et al., 2014b). That study also found that axenic *A. minutissimum* cultures mostly secrete soluble
59 carbohydrates while the presence of insoluble carbohydrates in xenic cultures coincided with the
60 appearance of capsules. This strengthened the argument that *A. minutissimum* capsules consist of
61 carbohydrates and are important for the inter-kingdom interactions of diatoms and bacteria.

62 Diatom capsules have puzzled phycologists for a long time and their potential physiological
63 and ecological function have elicited a variety of hypotheses (Lewin, 1955; Geitler, 1977). For
64 example, capsules have been proposed to participate in locomotion, flotation, attachment, waste
65 removal, catchment of inorganic nutrients, storage of polysaccharides, sexual reproduction, as
66 well as protection against grazing and dehydration. More recently, it was demonstrated that
67 capsule formation is dependent on at least "a certain minimum light intensity", sparking the idea
68 that capsules might serve as an additional polysaccharide storage pool, once intracellular
69 capacities are saturated (Staats et al., 2000).

70 While diatom capsules have mostly been characterised biochemically, electron microscopical
71 analyses have so far focussed on the morphology of diatom frustules (Toyoda et al., 2005, 2006;
72 Morin, Coste & Hamilton, 2008) and the development of its morphological variations as
73 environmental markers (Potapova & Hamilton, 2007; Hlúbková, Ector & Hoffmann, 2011;
74 Cantonati et al., 2014). In the present study, scanning electron microscopy (SEM), as well as

75 energy-dispersive X-ray (EDX) spectroscopy were employed to analyse the microstructure and
76 development stages of *Achnanthidium minutissimum* capsules in order to further develop this
77 species as a model system for diatom-bacteria interactions, and to elucidate one aspect of the
78 complex interactions of diatoms and other micro-organisms.

79 Materials & Methods

80 Cultivation conditions

81 *Achnanthidium minutissimum* (Kützing) Czarnecki (previously called
82 *Achnanthes minutissima*) strains previously isolated from benthic biofilms of Lake Constance
83 were cultivated as described (Windler et al., 2014b). In order to grow diatom biofilms directly on
84 sample carriers for scanning electron microscopy, 6- (instead of 48)-well plates (Sarstedt, USA,
85 order number 83.1839.500) were used. Sample carrier disks of ca. 1 cm in diameter were
86 punched from Thermanox tissue culture cover slips (Miles Laboratories Inc., USA). Because the
87 Thermanox material has two different sides, care was taken to always store and handle the disks
88 right-side-up. Because autoclavation proved to melt them, sterilisation was instead conducted by
89 immersion in 70% isopropanol (v/v in H₂O) over night and subsequent irradiation with UV light
90 for 2 h in a laminar flow cabinet. Sterile disks were placed into the wells and covered with 3 to
91 5 mL of modified Bacillariophycean Medium (BM; (Schlösser, 1994; Windler, Gruber & Kroth,
92 2012). Well areas may allow for the parallel cultivation of several disks, but due to the risk of
93 them sliding on top of one another, placing only a single disk into each well is recommended.
94 Culture wells were inoculated with 5×10⁵ to 1×10⁶ *A. minutissimum* cells in 3 to 5 ml BM. Cells
95 were confirmed to be axenic or xenic by SYBR Green staining. Well plates were sealed with
96 Parafilm and incubated at 16°C under an illumination regime of 12 h dark and 12 h light at 20-
97 50 µmol photons×m⁻²×s⁻¹ for 11 to 31 days.

98 Crystal violet staining and bright-field microscopy

99 Thermanox disks were removed from stationary cultures after 11, 20 and 31 days with
100 inverted (“soldering” or “cover glass”) forceps (Hammacher, Germany) and rinsed with 1 mL
101 sterile-filtered tap water. A Gram-staining protocol adapted from Kaplan & Fine (2002) was
102 applied to visualise adherent cells and their extracellular polymeric structures as follows: A
103 droplet of 200 µL solution of 0.02% crystal violet (CV) in sterile filtered tap water was applied
104 onto the disk for 1-2 min, which was held suspended by forceps. Disks were rinsed with 1 to

105 3 mL water, until the run-off no longer contained visible CV. In order to find the same cell
106 clusters in both microscopic approaches, pointing or encircling scratches were made into the
107 biofilm-covered disk surfaces.

108 Disks were placed on moistened glass slides and moistened additionally with 20 μ L sterile-
109 filtered tap water. Cover slips were applied carefully and marked regions were observed under a
110 BX51 (Olympus, USA) microscope with bright-field using chlorophyll fluorescence filters.
111 Images of these areas at various magnifications were taken with AxioCams MRm and MRc using
112 AxioVision software (Zeiss, Germany). See figures 1 and 2 for results. Disks were recovered
113 from between glass slides and cover slips by separating the glass pieces with 1 mL of water.

114 **Scanning electron microscopy (SEM) and energy-dispersive X-ray 115 (EDX) spectroscopy**

116 Diatom cells on thermanox disks were fixed by incubation in a mixture of 2% glutaraldehyde,
117 10 mM CaCl₂ and 10 mM MgCl₂ in 0.1 M sodium cacodylate buffer at pH 7 and room
118 temperature for 2 h. Dehydration was conducted first with 30% and 50% EtOH, at room
119 temperature for 2 h each, followed by 70% EtOH at 4°C over night, 90% EtOH at room temp. for
120 2 h and finally with 96% and 100% EtOH twice for 1 h each. Critical point drying in CO₂
121 followed (Balzers CPD030, Liechtenstein) and samples were finally sputtered with gold and
122 palladium to a thickness of 5 nm (Balzers SCD030, Liechtenstein).

123 After fixation, dehydration and Au/Pd-sputtering, the biofilm-covered Thermanox disks were
124 imaged with a Zeiss “AURIGA” scanning electron microscope, controlled with the “SmartSEM”
125 software v05.04.05.00. See figures 2 to 6 for results. Energy-dispersive X-ray (EDX) spectra
126 were recorded with an Oxford Instruments “X-Max 20 mm²” device, controlled with the “INCA”
127 software v4.15. See figure 7 for results.

128 **Bacterial counting and statistical analyses**

129 Bacteria (rod-shaped particles) on fully visible *A. minutissimum* valve faces were counted in
130 scanning electron micrographs. Valve faces were classified into frustules and capsules, depending
131 on whether pores were visible or completely disappeared under layer of capsule material. Diatom
132 cells with partial encapsulation were not included in the counting, and neither were bacteria cells
133 which attached to the girdle bands of diatom cells.

134 ImageJ v1.46r with the Cell Counter plug-in v2010/12/07 was used to count diatoms and
135 bacteria cells. This data was evaluated in the R environment for statistical computing v3.1.1 and
136 RStudio v0.98. See figure 8 for results.

137 **Results and Discussion**

138 Xenic *Achnanthidium minutissimum* were grown on disks of ca. 1 cm diameter punched from
139 Thermanox tissue culture cover slips. These disks were used both for bright-field light and
140 scanning electron microscopy to correlate the appearance of hydrated capsules with their
141 microstructure after dehydration.

142 After an incubation period of 11 days, thermanox disk surfaces were densely covered by a
143 mono-layer of xenic *A. minutissimum* cells (Fig. 1). The biofilm was visible as light greenish-
144 brown coloration on the substrate disks. Staining with the dye crystal-violet (CV) and subsequent
145 bright-field microscopy showed that large portions of the diatom cells were surrounded by
146 capsules, which absorbed the chlorophyll fluorescence (chl).

147 In contrast, axenic *A. minutissimum* cells did not form biofilms on the substrate disks, so that
148 careful rinsing already removed most of the cells. This observation is in agreement with studies
149 that utilised other growth substrates to compare biofilm formation by axenic and xenic diatom
150 cultures. By measuring chlorophyll (chl) contents, the possibility that axenic cells might simply
151 be less proliferate was excluded (Windler et al., 2014b). Xenic *A. minutissimum* cultures on the
152 other hand have also been found to develop biofilms on glass beads as well as in plastic multi-
153 well plates (Lubarsky et al., 2010; Windler et al., 2014b). Our results therefore demonstrate, that
154 *A. minutissimum* biofilms can easily be grown on thermanox disks, enabling direct preparation
155 for electron microscopy of native biofilm samples.

156 **Identification of *A. minutissimum* capsule microstructures**

157 In order to correlate the hydrated *A. minutissimum* capsules visible in light microscopy to their
158 dehydrated appearance in SEM, areas were marked by scratches on the crystal violet (CV)
159 stained disks and cells of interest were identified by bright-field microscopy (BFM).
160 Subsequently, the same cells were observed by scanning electron microscopy (SEM; Fig. 2). In
161 BFM, the CV stained capsules were visible as balloon-like structures around most of the cells. As
162 extracellular polymeric structures in the genus *Achnanthidium* are composed mostly of
163 carbohydrates (Wustman et al., 1998), strong hydration in the native biofilm is likely the source

164 of this appearance of capsules. In SEM, however, we were able to distinguish two types of
165 *A. minutissimum* cells in xenic biofilms already at low magnifications: cells with pores in their
166 frustules still visible, and cells covered by an apparently unstructured material masking the pores.

167 The frustules of non-encapsulated xenic, as well as axenic *A. minutissimum* cells appeared
168 identical to those from scanning electron micrographs shown in previous studies (Mayama &
169 Kobayasi, 1989; Potapova & Hamilton, 2007; Hlúbková, Ector & Hoffmann, 2011). The low
170 prevalence of raphes in our images is most likely due to the orientation of raphes towards the
171 substrate for mucilage secretion (Gordon & Drum, 1970, p. 197; Wetherbee et al., 1998). Natural
172 attachment and orientation of cells on our biofilm disks was retained because we did not employ
173 harsh preparation techniques, such as boiling diatom cells in sulphuric acid (Mayama &
174 Kobayasi, 1989). Such harsh treatments are designed to prepare only frustules and would in our
175 case have resulted in cell detachment from the growth substrate and random orientation on the
176 SEM sample carrier. We however, applied the final SEM sample carrier disks directly as growth
177 substrates for the biofilms.

178 The SEM images in figure 3 show that the capsule material appears to be unstructured,
179 resembling the “adhering film and tube” of *Cymbella microcephala* and *Cymbella prostrata*
180 reported in figures 31 & 32 of Hoagland et al. (1993).

181 Closer inspection provided many examples that the frustules of non-encapsulated xenic
182 *A. minutissimum* cells were not be completely free of extracellular polymeric substances (EPS).
183 Instead, they were covered by a mesh of fibrils (Fig. 3B), arranged mostly around the frustule
184 pores, sometimes crossing them and sometimes sticking out. The average diameter of these fibrils
185 was about 45 ± 9 nm. The fibrils were rarely observed to be secreted through the pores, although
186 these were found to be large enough (from 60 to 140 nm in diameter), showing round to elongated
187 shapes. Fibrils were generally longer than pores where in diameter, but quantification was not
188 performed because branching and crossing points made it infeasible to determine the respective
189 beginnings or ends. Similarly structured, thinner fibrils were reported previously only for marine
190 diatoms (Bosak et al., 2012). To the best of our knowledge, this is the first report of frustule-
191 attached fibril structures in fresh water diatoms.

192 The dehydrated capsule material displayed a slight granularity in scanning electron
193 micrographs (Fig. 3C), but unlike on frustules (with or without fibrils) few distinct features were
194 apparent. The capsule material appears to be similar to the shaft ultra-structure of the marine
195 diatom *Achnanthes longipes* displayed in figure 8 of Wang et al. (2000). Material secretion was

196 observed to appear in apical pore fields; the site of pad and stalk formation (Wang et al., 2000).
197 Although originally reported for that marine diatom by (Wustman et al., 1998), we observed this
198 also on the rapheless epitheca of the fresh water diatom *A. minutissimum*.

199 In addition to covering the cells, the capsule material also had sheet-like structures (arrows in
200 figure 3A) in portions stretched between *A. minutissimum* cells and the anchoring points on the
201 substrate. This pattern is most likely due to dehydration during SEM sample preparation
202 (Hoagland et al., 1993). Due to fixation of the samples prior to drying, the hydrated capsules
203 most likely shrank in their entirety to the dehydrated, envelope-like structures.

204 **Fibrillar precursors may give rise to *A. minutissimum* capsules**

205 In order to elucidate the process of capsule formation, we analysed the observed cell surface
206 morphologies more closely. We found intermediate stages between the fibrillar meshes that only
207 partially covered the frustule surface and the complete encapsulation with apparently
208 unstructured material (Fig. 4).

209 Fibrillar meshes of varying densities were detected in both axenic and xenic cultures during
210 the stationary phase. Axenic cultures additionally contained cells with even fewer and shorter
211 fibrils than displayed in figure 4A. This indicates that there is a bias introduced by washing the
212 substrate disks prior to SEM preparation. Probably only those axenic cells possessing at least a
213 minimum amount of EPS on their surface were able to adhere to the disks. In xenic cultures,
214 bacteria likely induced the secretion of EPS (Bruckner et al., 2011) and thus substrate adherence
215 by the majority of cells. This is in line with the observation that capsules were only found in
216 xenic cultures, particularly later in the stationary phase.

217 Based on the visual impression, we think that the dense fibrillar meshes represent precursors
218 of the mature capsules. For example, the disordered arrangement of fibrils shown in figure 4B is
219 also a feature of the unstructured capsule material. In it, no particular order of the slightly
220 granular substructures is discernible either (Fig. 4C). An alternative explanation for the capsule
221 structure may be the polymerisation of a secondary type of fibrils upon the primary mesh
222 (Fig. 4A), relegating the latter to a scaffolding function.

223 In order to elucidate whether or not fibrils and capsules might be related, we observed
224 mechanically stressed capsule areas (Fig. 5). Here, tension yielded an alignment of capsule
225 micro-structures, as well as fraying on the edges. Fibrillar structures resulting from these
226 processes were similar in diameter to the fibrils covering the frustules.

227 There are two possible sources for the mechanical force. Motility of the cells relative to each
228 other in the native biofilm could induce force. However, it has been reported for a related species
229 in the order *Achnanthales*, that a loss of motility following the production of EPS structures
230 occurs (Wang et al., 1997). It is therefore also possible that mechanical force could be caused by
231 the dehydration during SEM sample preparation. Both explanations lead to the question why
232 mechanical force highlighted the fibrillar microstructure, while relaxed capsule areas (see
233 previous figures) appeared unstructured.

234 Inter-fibril cross-linkage by for example hydrogen bonds was apparently weaker than intra-
235 fibril connections, which are likely of covalent nature. Also, the integrity of fibrillar building
236 blocks was apparently preserved during capsule formation. Otherwise, mechanical force would
237 likely have favoured shearing of fibrillar microstructures over re-emergence from the capsule
238 material.

239 We therefore suggest fibrils as a precursor candidate for capsules, into which they may
240 condense as depicted in figure 4, for example by enzymatic cross-linking or transglycosylase
241 activity. Fibrils may be disguised in relaxed capsule material because they are arranged in a
242 disorderly fashion, but mechanical stress may yield a visible alignment. Micromanipulation
243 experiments that artificially apply mechanical force to encapsulated cells in the native biofilm
244 should be developed to investigate this possibility further.

245 Capsule material does not contain silica

246 In order to exclude the possibility that the capsule structures we observed might be frustule
247 deformations or extensions, two further experiments were conducted. First, because stress-
248 induced frustule deformations (Cantonati et al., 2014; Windler et al., 2014a) might also result in
249 the disappearance of pores, we imaged frustules at a higher excitation voltage (10 instead of
250 5 keV; Fig. 6), resulting in translucency of some capsule regions. This way, frustule pores beyond
251 thicker capsule material became visible, demonstrating that capsules are an additional layer of
252 material around the frustule.

253 Secondly, capsule material was screened for the presence of silicon (Si). This chemical
254 element is a major component of diatom frustules, in which it is present as hydrated silicon
255 dioxide. Capsules on the other hand may consist mostly of extracellular polymeric carbohydrates
256 (Windler et al., 2014b). Energy-dispersive X-ray (EDX) spectra were therefore recorded from
257 capsule areas with and without a frustule below them (Fig. 7).

258 As expected, Si signals around 1.75 keV were obtained from control areas with frustule
259 material below the capsules (Guerra et al., 2013; Chandrasekaran et al., 2014). Si signals were 2.5
260 to 12 times stronger from such control areas than from capsule material only. We can therefore
261 exclude the possibility that *A. minutissimum* capsule material is some kind of frustule extension
262 or deformation.

263 Low Si counts (black line in grey highlighted area in figure 7) are likely contributed by the
264 frustule edges in close proximity due to the “pear effect” (Arnould & Hild, 2007). It explains,
265 how excited electrons diffuse into the sample, so that a pear-shaped volume of ca. 0.5-1 μm
266 diameter below the measurement point or area also emits detectable X-rays. The cell bodies in
267 figure 7 are separated by approximately that distance. The stronger gold (Au) signal around
268 2.15 keV most likely resulted from the larger sputtered surface area within the measurement
269 volume.

270 Because no notable nitrogen signals (N; 0.39 keV) were recorded from the capsule material,
271 we tentatively exclude chitin as a major capsule building block candidate. Chitin fibrils have been
272 found to be secreted by diatoms into the surrounding water body (Gardner & Blackwell, 1971;
273 Herth, 1979). In contrast, the fibrillar meshes we describe here, tightly covered the frustule
274 surfaces of individual *A. minutissimum* cells and therefore likely represent different EPS
275 structures.

276 **Bacteria preferentially attach to encapsulated diatom cells**

277 It has been proposed that *A. minutissimum* capsules might be an asset in the mutualistic
278 relationship of the diatom with its satellite bacteria (Windler et al., 2014b). Previous findings
279 suggest a pattern of bacterial attachment to xenic *A. minutissimum* cells that would support this
280 hypothesis (Windler, Gruber & Kroth, 2012) as diatom cells seemingly are surrounded by a
281 bacteria-free space, followed by a layer of densely aggregated bacteria cells. Although no CV
282 stains were conducted in that study, the bacteria free regions resemble the EPS structures reported
283 as capsules.

284 It became apparent during the analyses of SEM images, that diatom-attached bacteria cells
285 occurred more often on capsules than on frustules. To substantiate this observation, bacteria cells
286 were counted on both diatom cell surface types (Fig. 8).

287 Notably higher numbers of bacteria (ca. 25 times more on average) were attached to capsules
288 as compared to frustules throughout the stationary phase (means: 11.41 ± 8.23 and 0.46 ± 0.82

289 respectively). As figure 8 shows, the variance in the numbers of bacteria per diatom (black dots)
290 was larger (ca. 100 times) on encapsulated cells than on frustules, indicating that not all
291 encapsulated *A. minutissimum* cells were equally strongly colonised by bacteria.

292 Bacterial cells as well as non-encapsulated diatom cells were able to individually retain
293 attachment to the substrate during SEM sample preparation. The lower prevalence of bacteria
294 attached to frustules is therefore probably not due to lower ability of the bacteria to remain
295 attached to frustules during SEM sample preparation. Instead, the bacteria preferred capsules
296 over frustules.

297 It is possible that diatom capsules serve as a common nutrient pool to some of the diatom's
298 satellite bacteria in a mutualistic relationship (Bruckner et al., 2008). In bacterial biofilms,
299 nutrient distribution is predominantly determined by diffusion, sometimes along strong gradients
300 within a biofilm (Stewart, 2003). Similarly, variations of cellular nutrient distributions within
301 fresh water diatom biofilms exist (Murdock et al., 2010). Therefore, competition between
302 individual diatom cells for re-mineralising bacteria could occur. Nutrient-limited, but still
303 photosynthetically active diatom cells may produce predominantly insoluble carbohydrates to
304 foster close attachment of heterotrophic bacteria that re-mineralise EPS or secrete vitamins.
305 Axenic *A. minutissimum* cultures have been shown to secrete carbohydrates predominantly in
306 soluble form (Windler et al., 2014b). The same may be true for individual *A. minutissimum* cells
307 under non-limiting nutrient conditions, despite being embedded in a xenic biofilm.

308 Our finding that bacteria attach preferentially to capsules strengthens the argument that
309 capsules play a role in the inter-kingdom relationship of satellite bacteria and benthic diatoms.
310 Whether this relationship is antagonistic, mutualistic or commensal in nature remains to be
311 elucidated. Labelling experiments with isotopes or fluorophores may assist in the determination
312 of carbohydrate fluxes from the diatom's EPS structures to bacteria feeding on those.

313 Acknowledgements

314 We thank Joachim Hentschel, Lauretta Nejedli and Michael Laumann of the Electron
315 Microscopy Center of the University of Konstanz for sample preparation, SEM and EDX device
316 operations, and insightful discussions, as well as Ansgar Gruber and Carolina Rio Bartulos for
317 helpful ideas and suggestions.

318 **References**

Arnould O, Hild F. 2007. On the measurement by EDX of diffusion profiles of Ni/Cu assemblies. *arXiv:0712.3636 [physics]*.

Bahulikar RA. 2006. Diatoms from littoral zone of Lake Constance: diversity, phylogeny, extracellular polysaccharides and bacterial associations.

Bell WH, Lang JM, Mitchell R. 1974. Selective stimulation of marine bacteria by algal extracellular products. *Limnology and Oceanography* 19:833–839.

Bosak S, Pletikapić G, Hozić A, Svetličić V, Sarno D, Viličić D. 2012. A Novel Type of Colony Formation in Marine Planktonic Diatoms Revealed by Atomic Force Microscopy. *PLoS ONE* 7:e44851.

Bradbury J. 2004. Nature's Nanotechnologists: Unveiling the Secrets of Diatoms. *PLoS Biol* 2:e306.

Bruckner CG, Bahulikar R, Rahalkar M, Schink B, Kroth PG. 2008. Bacteria Associated with Benthic Diatoms from Lake Constance: Phylogeny and Influences on Diatom Growth and Secretion of Extracellular Polymeric Substances. *Applied and Environmental Microbiology* 74:7740–7749.

Bruckner CG, Kroth PG. 2009. Protocols for the Removal of Bacteria from Freshwater Benthic Diatom Cultures1. *Journal of Phycology* 45:981–986.

Bruckner CG, Rehm C, Grossart H, Kroth PG. 2011. Growth and release of extracellular organic compounds by benthic diatoms depend on interactions with bacteria. *Environmental Microbiology* 13:1052–1063.

Buhmann M, Kroth PG, Schleheck D. 2012. Photoautotrophic–heterotrophic biofilm communities: a laboratory incubator designed for growing axenic diatoms and bacteria in defined mixed-species biofilms. *Environmental Microbiology Reports* 4:133–140.

Cantonati M, Angeli N, Virtanen L, Wojtal AZ, Gabrieli J, Falasco E, Lavoie I, Morin S, Marchetto A, Fortin C et al. 2014. *Achnanthidium minutissimum* (Bacillariophyta) valve deformities as indicators of metal enrichment in diverse widely-distributed freshwater habitats. *Science of The Total Environment* 475:201–215.

Chandrasekaran S, Sweetman MJ, Kant K, Skinner W, Losic D, Nann T, Voelcker NH. 2014. Silicon diatom frustules as nanostructured photoelectrodes. *Chemical Communications* 50:10441–10444.

Cyr H, Morton KE. 2006. Distribution of biofilm exopolymeric substances in littoral sediments of Canadian Shield lakes: the effects of light and substrate. *Canadian Journal of Fisheries and Aquatic Sciences* 63:1763–1776.

Czarnecki DB, Edlund MB. 1995. Combinations for Some Taxa of Achnanthes. *Diatom Research* 10:207–209.

Daniel GF, Chamberlain AHL, Jones EBG. 1987. Cytochemical and electron microscopical observations on the adhesive materials of marine fouling diatoms. *British Phycological Journal* 22:101–118.

Field CB, Behrenfeld MJ, Randerson JT, Falkowski P. 1998. Primary Production of the

Biosphere: Integrating Terrestrial and Oceanic Components. *Science* 281:237–240.

Gardner KH, Blackwell J. 1971. The substructure of crystalline cellulose and chitin microfibrils. *Journal of Polymer Science Part C: Polymer Symposia* 36:327–340.

Geitler L. 1932. Der Formwechsel der pennaten Diatomeen (Kieselalgen). *Arch Protistenk* 78:1–226.

Geitler L. 1977. Entwicklungsgeschichtliche Eigentümlichkeiten einiger Achnanthes-Arten (Diatomeae). *Plant Systematics and Evolution* 126:377–392.

Gordon R, Drum RW. 1970. A Capillarity Mechanism for Diatom Gliding Locomotion. *Proceedings of the National Academy of Sciences* 67:338–344.

Guerra MBB, Schaefer CEGR, Carvalho GGA de, Souza PF de, Júnior DS, Nunes LC, Krug FJ. 2013. Evaluation of micro-energy dispersive X-ray fluorescence spectrometry for the analysis of plant materials. *Journal of Analytical Atomic Spectrometry* 28:1096–1101.

Herth W. 1979. The site of β -chitin fibril formation in centric diatoms. II. The chitin-forming cytoplasmic structures. *Journal of Ultrastructure Research* 68:16–27.

Hlúbíková D, Ector L, Hoffmann L. 2011. Examination of the type material of some diatom species related to *Achnanthidium minutissimum* (Kütz.) Czarn. (Bacillariophyceae). *Algological Studies* 136:19–43.

Hoagland KD, Rosowski JR, Gretz MR, Roemer SC. 1993. Diatom Extracellular Polymeric Substances: Function, Fine Structure, Chemistry, and Physiology. *Journal of Phycology* 29:537–566.

Johnson RE, Tuchman NC, Peterson CG. 1997. Changes in the Vertical Microdistribution of Diatoms within a Developing Periphyton Mat. *Journal of the North American Benthological Society* 16:503–519.

Kaplan JB, Fine DH. 2002. Biofilm Dispersal of *Neisseria subflava* and Other Phylogenetically Diverse Oral Bacteria. *Applied and Environmental Microbiology* 68:4943–4950.

Krammer K, Lange-Bertalot H. 1991. *Stüßwasserflora von Mitteleuropa, Bacillariophyceae. Achnanthaceae. Kritische Ergänzungen zu Navicula (Lineolatae) und Gomphonema*. Gustav Fischer Verlag, Stuttgart.

Lewin JC. 1955. The Capsule of the Diatom *Navicula pelliculosa*. *Journal of General Microbiology* 13:162–169.

Lubarsky HV, Hubas C, Chchoolek M, Larson F, Manz W, Paterson DM, Gerbersdorf SU. 2010. The Stabilisation Potential of Individual and Mixed Assemblages of Natural Bacteria and Microalgae. *PLoS ONE* 5:e13794.

MacDonald JD. 1869. On the structure of the Diatomaceous frustule, and its genetic cycle. *The Annals and Magazine of Natural History* 3:1–8.

Mann DG. 1999. The species concept in diatoms. *Phycologia* 38:437–495.

Mayama S, Kobayasi H. 1989. Sequential Valve Development in the Monoraphid Diatom *Achnanthes Minutissima* Var. *Saprophila*. *Diatom Research* 4:111–117.

Molino PJ, Wetherbee R. 2008. The biology of biofouling diatoms and their role in the development of microbial slimes. *Biofouling* 24:365–379.

Morin S, Coste M, Hamilton PB. 2008. Scanning Electron Microscopy Observations of

Deformities in Small Pennate Diatoms Exposed to High Cadmium Concentrations 1. *Journal of Phycology* 44:1512–1518.

Murdock JN, Dodds WK, Reffner JA, Wetzel DL. 2010. Measuring Cellular-Scale Nutrient Distribution in Algal Biofilms with Synchrotron Confocal Infrared Microspectroscopy. *Spectroscopy* 25:32–41.

Myklestad S, Holm-Hansen O, Vårum KM, Volcani BE. 1989. Rate of release of extracellular amino acids and carbohydrates from the marine diatom *Chaetoceros affinis*. *Journal of Plankton Research* 11:763–773.

Patrick R, Reimer CW. 1966. *The diatoms of the United States*. Academy of Natural Sciences.

Pfitzer E. 1871. *Untersuchungen über Bau und Entwicklung der Bacillariaceen (Diatomaceen)*.

Potapova M, Hamilton PB. 2007. Morphological and Ecological Variation Within the *Achnanthidium Minutissimum* (bacillariophyceae) Species Complex. *Journal of Phycology* 43:561–575.

Schlösser UG. 1994. SAG - Sammlung von Algenkulturen at the University of Göttingen Catalogue of Strains 1994. *Botanica Acta* 107:113–186.

Staats N, Stal LJ, Winder B de, Mur LR. 2000. Oxygenic photosynthesis as driving process in exopolysaccharide production of benthic diatoms. *Marine Ecology Progress Series* 193:261–269.

Stewart PS. 2003. Diffusion in Biofilms. *Journal of Bacteriology* 185:1485–1491.

Toyoda K, Idei M, Nagumo T, Tanaka J. 2005. Fine-structure of the vegetative frustule, perizonium and initial valve of *Achnanthes yaquinensis* (Bacillariophyta). *European Journal of Phycology* 40:269–279.

Toyoda K, Williams DM, Tanaka J, Nagumo T. 2006. Morphological investigations of the frustule, perizonium and initial valves of the freshwater diatom *Achnanthes crenulata* Grunow (Bacillariophyceae). *Phycological Research* 54:173–182.

Wang Y, Chen Y, Lavin C, Gretz MR. 2000. Extracellular matrix assembly in diatoms (Bacillariophyceae). iv. ultrastructure of *Achnanthes longipes* and *Cymbella cistula* as revealed by high-pressure freezing/freeze substituton and cryo-field emission scanning electron microscopy. *Journal of Phycology* 36:367–378.

Wang Y, Lu J, Mollet JC, Gretz MR, Hoagland KD. 1997. Extracellular Matrix Assembly in Diatoms (Bacillariophyceae) II. 2,6-Dichlorobenzonitrile Inhibition of Motility and Stalk Production in the Marine Diatom *Achnanthes longipes*. *Plant Physiology* 113:1071–1080.

Wetherbee R, Lind JL, Burke J, Quatrano RS. 1998. Minireview—The first kiss: Establishment and control of initial adhesion by raphid diatoms. *Journal of Phycology* 34:9–15.

Widdows J, Brinsley M. 2002. Impact of biotic and abiotic processes on sediment dynamics and the consequences to the structure and functioning of the intertidal zone. *Journal of Sea Research* 48:143–156.

Windler M, Bova D, Kryvenda A, Straile D, Gruber A, Kroth PG. 2014a. Influence of bacteria on cell size development and morphology of cultivated diatoms. *Phycological Research*.

Windler M, Gruber A, Kroth PG. 2012. Purification of benthic diatoms from associated bacteria using the antibiotic imipenem. *Journal of Endocytobiosis and Cell Research* 22:62 – 65.

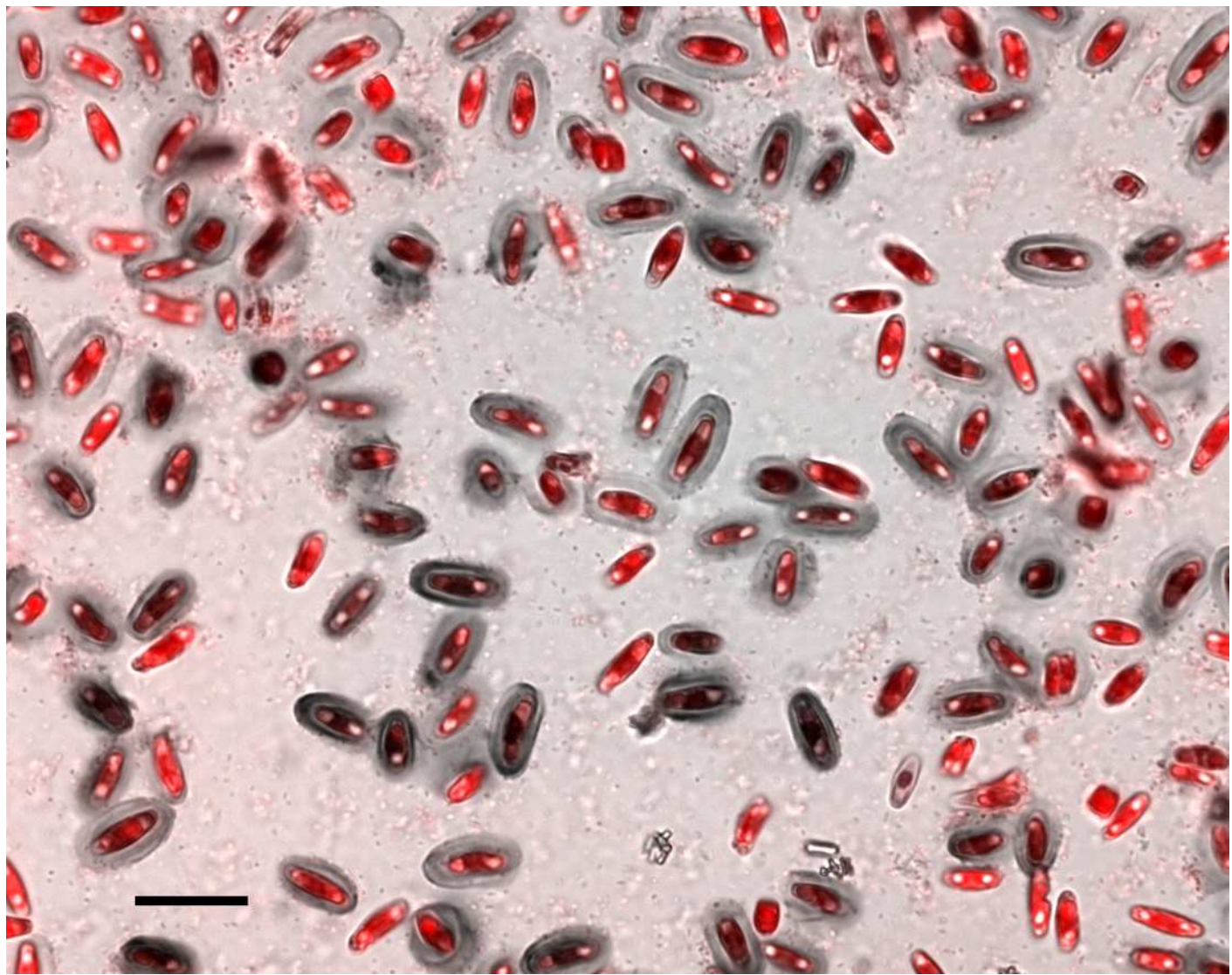
Windler M, Leinweber K, Rio Bartulos C, Philipp B, Peter G. K. 2014b. Bacterial Influence on Diatoms from Photoautotrophic Freshwater Biofilms (Chapter 4: Biofilm and capsule formation of the diatom *Achnanthidium minutissimum* are strongly affected by a bacterium). University of Konstanz.

Wustman BA, Lind J, Wetherbee R, Gretz MR. 1998. Extracellular Matrix Assembly in Diatoms (Bacillariophyceae) III. Organization of Fucoglucuronogalactans within the Adhesive Stalks of *Achnanthes longipes*. *Plant Physiology* 116:1431–1441.

1

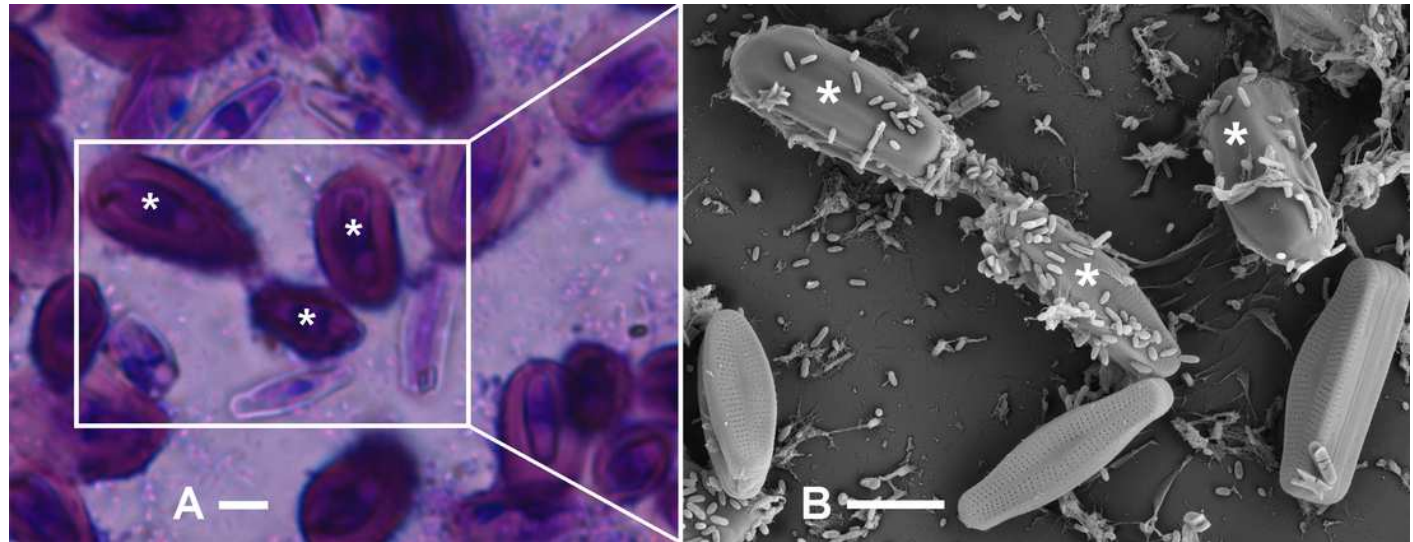
Chlorophyll fluorescence image (red) merged with the bright-field image of crystal violet (CV) stain (grey) of a xenic *A. minutissimum* biofilm after 11 days of incubation (scale: 20 μm).

Bacteria are visible as dark speckles between the diatom cells. The dark grey, balloon-like structures surrounding the diatom cells and absorbing chlorophyll fluorescence are capsules, as visualised in real colours in figure 2A.



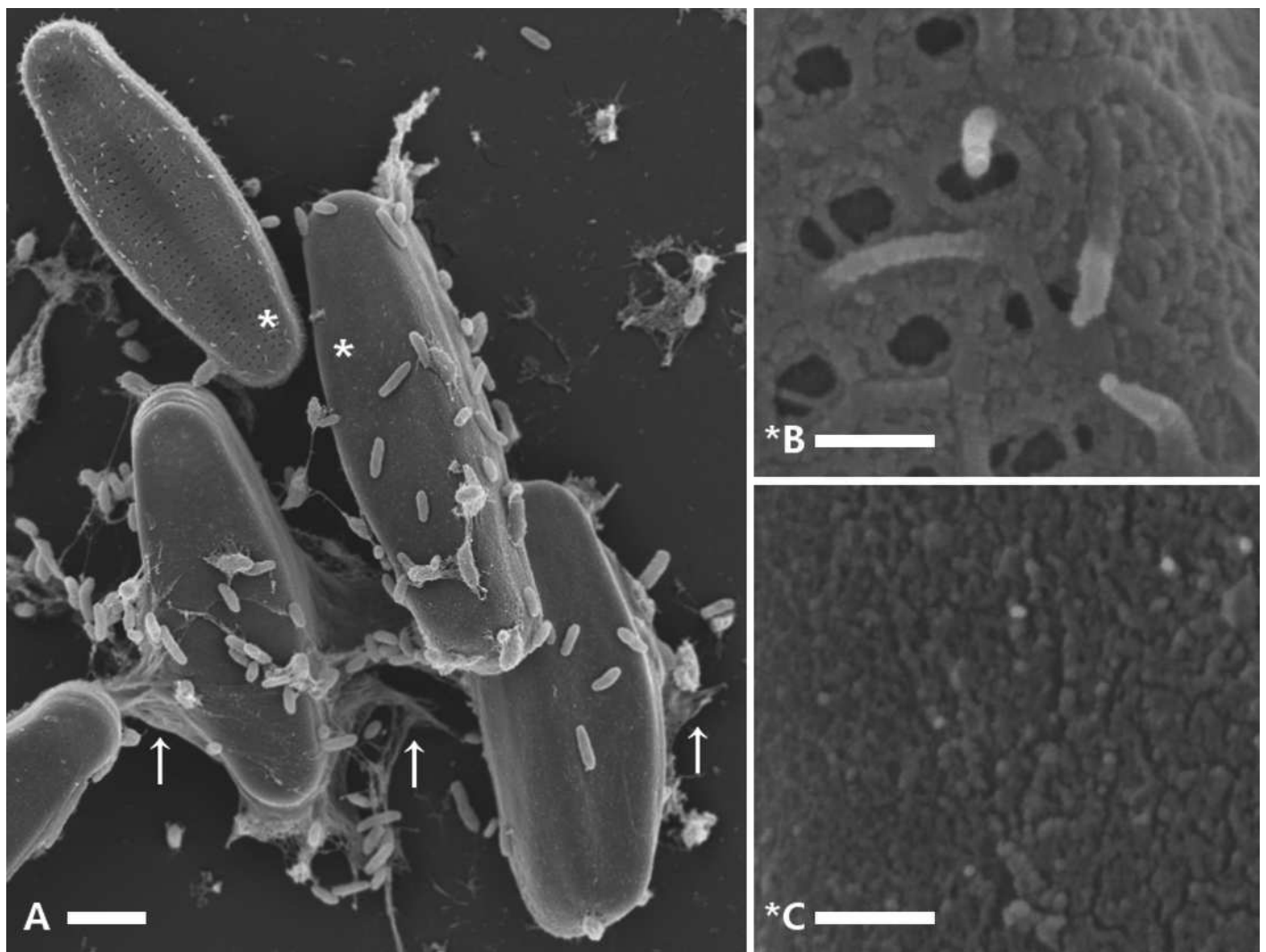
Identification of *A. minutissimum* capsules (asterisks) by subsequent observation of identical cell clusters in bright-field (A) and scanning electron (B) micrograph (scales: 5 μm).

A: 30 days old xenic *A. minutissimum* biofilm stained with crystal violet (CV). Encapsulated cells are strongly stained, while weak staining indicates a lack of extracellular polymeric substances (EPS) on the frustule surfaces. **B:** In the same cell cluster, encapsulated cells (asterisks) are surrounded by an opaque material. Frustule pores and raphe typical for *A. minutissimum* are only visible on cells that did not possess a capsule in the hydrated biofilm. Note also the unequal distribution of bacteria cells onto capsule material versus non-encapsulated frustules.

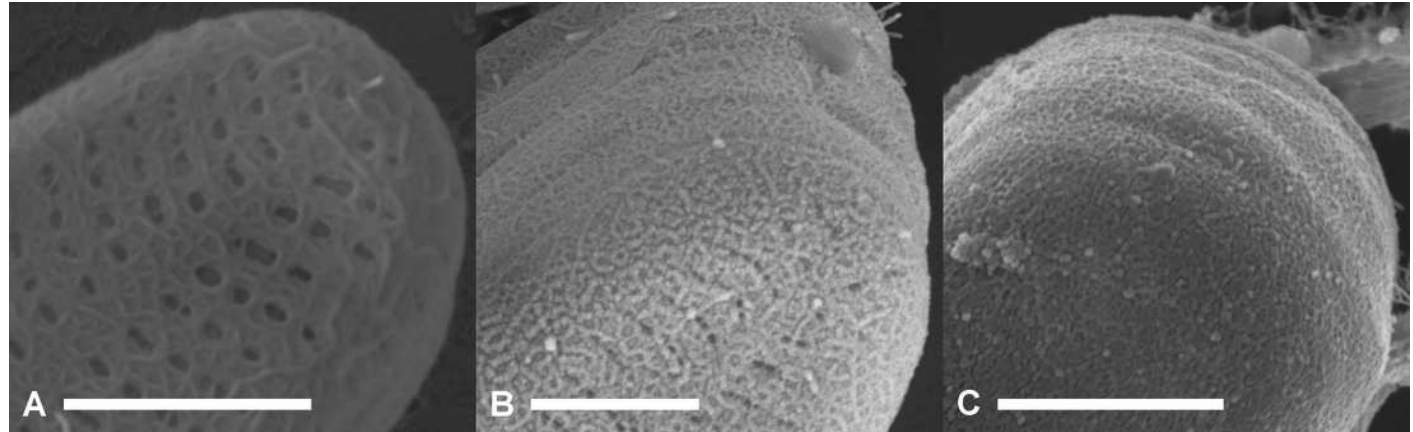


Comparison of microstructures on *A. minutissimum* cell surfaces in early stationary, xenic culture.

A (scale: 2 μ m): Capsule material is sometimes stretched between cells and/or towards the substrate (arrows). Asterisks denote magnified areas B and C. **B** (scale: 1 μ m): Non-encapsulated cells possess a fibrillar mesh of varying degrees of density. Frustule pores are only partially covered and in some cases, fibrils stick out from the frustule. **C** (scale: 1 μ m): Encapsulated cells are completely covered with a material that lacks clearly discernible structure, despite some granularity.

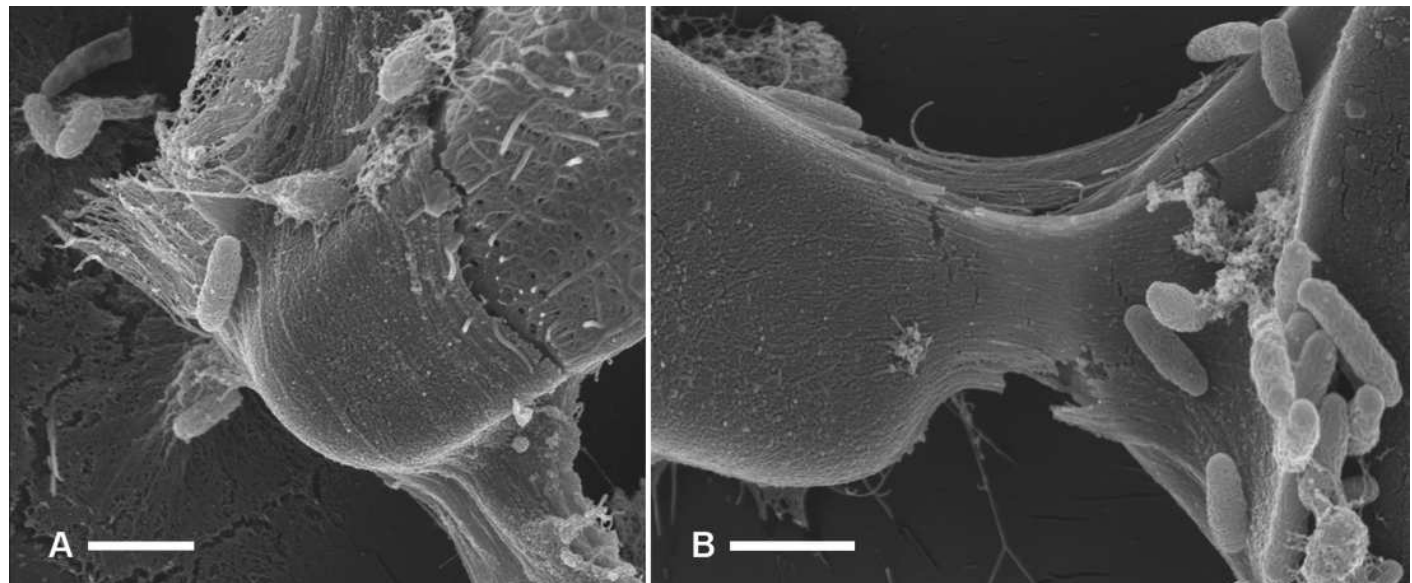


Fibrillar meshes (A) may form capsule material (C) by denser growth and cross-linking (B) of fibrils in xenic *A. minutissimum* cultures (scales: 1 μ m).



Capsule material reveals fibrillar composition under mechanical stress (scale bars = 1 μm).

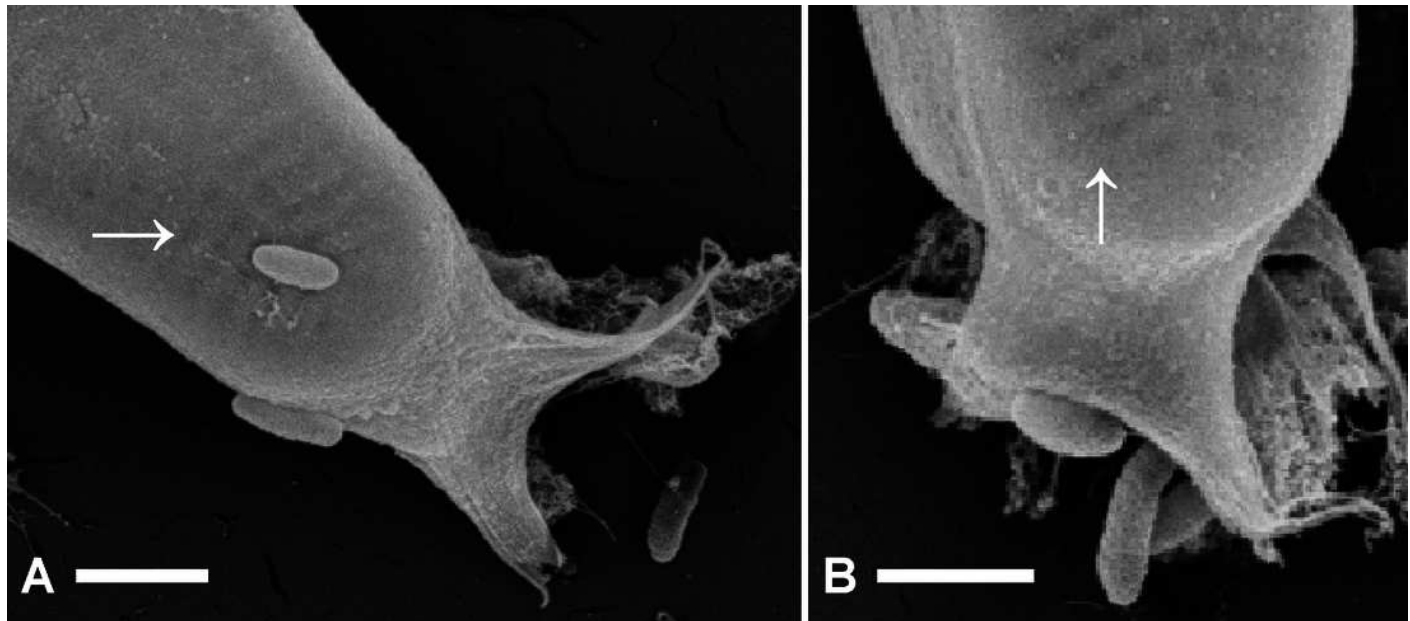
A: Tip of a partially encapsulated *A. minutissimum* cell with continuous fibrillar substructures within the capsule material. **B:** Capsule material stretched between cells reveal fibrillar microstructures.



6

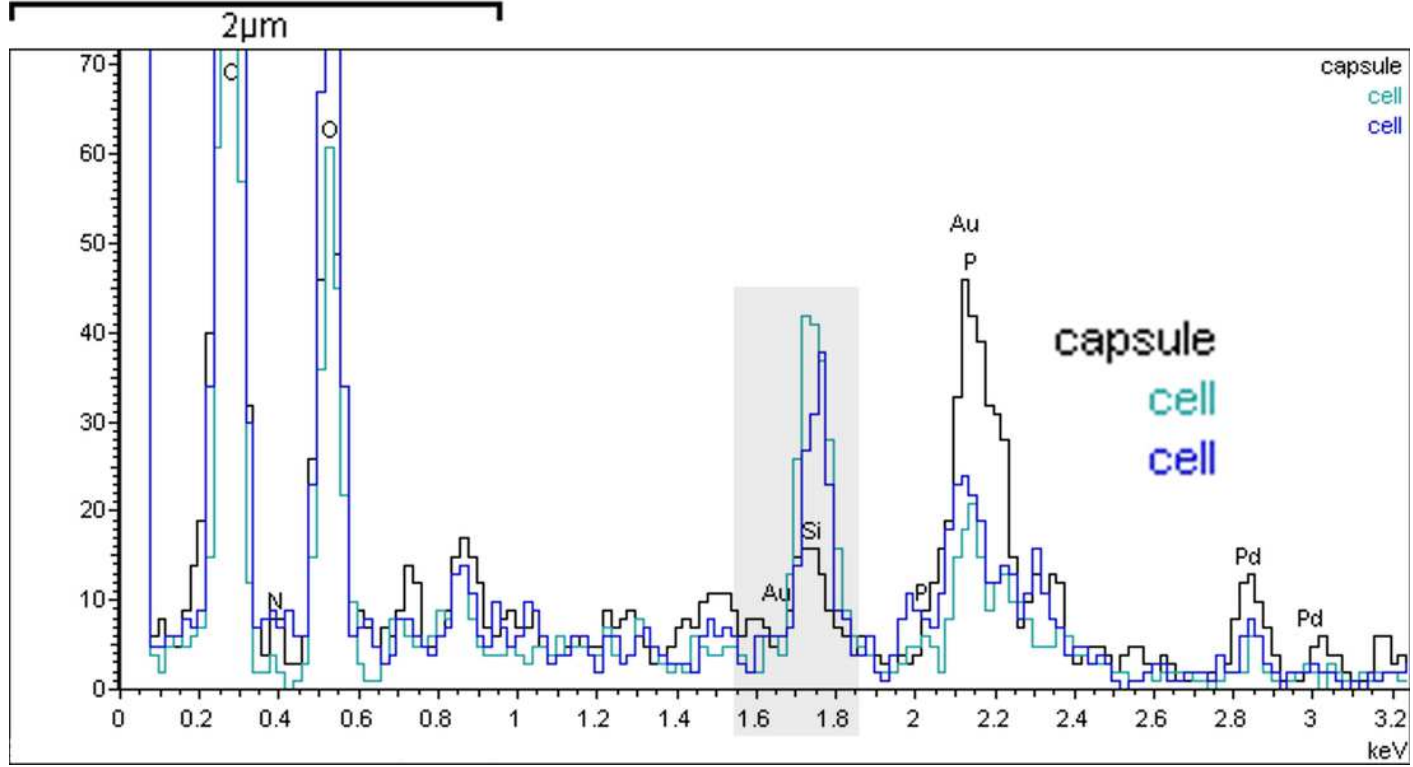
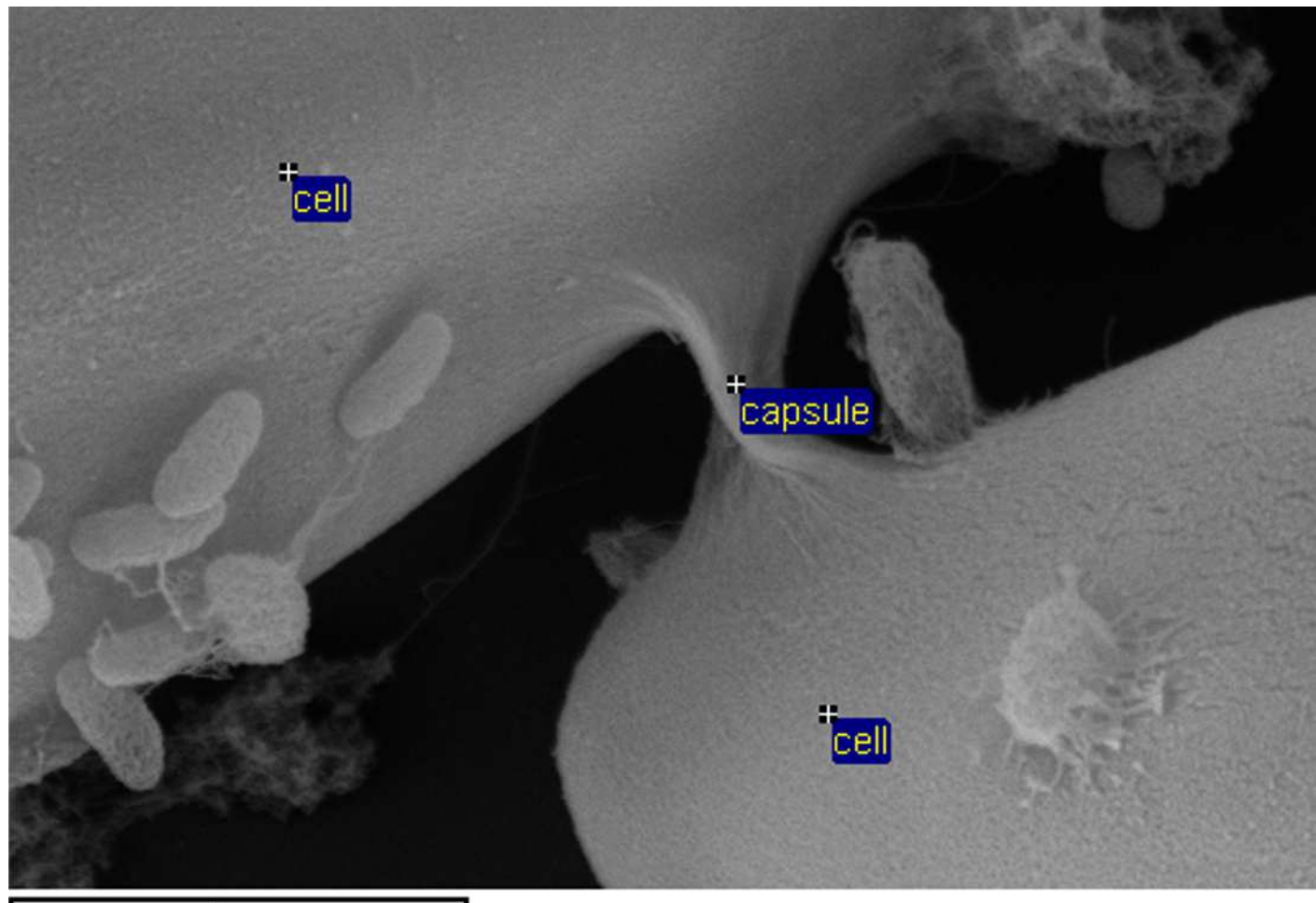
Capsule material around xenic *A. minutissimum* cells becomes translucent at increased excitation voltages (scales = 1 μ m).

Frustule pores are visible below the capsule material (arrows).



Scanning electron micrograph and energy-dispersive X-ray spectrum of early stationary, xenic *A. minutissimum* cells.

Less silicon (highlighted signal around 1.75 keV) is found in the capsule material (black trace) compared to the frustules (blue and turquoise traces; axis: x = keV, y = counts).



Box plot of the number of attached bacteria cells per frustule or capsule in stationary, xenic *A. minutissimum* cultures.

Dark grey boxes represent first and third quartile. White lines in box centres represent medians. Diamond symbols represent means. Dots represent individual counts of attached bacteria per diatom (larger dots are outliers). Bacteria were counted, if they were in direct, visible contact with the valve face of either a frustule, or a completely encapsulated diatom cell (see figures 2B and 3A for illustration). More capsules than frustules were counted, because more encapsulated diatom cells were present in our samples.

